A review of thermographic techniques for damage investigation in composites

Laura Vergani, Chiara Colombo, Flavia Libonati
Politecnico di Milano, Department of Mechanical Engineering, Via La Masa 1, 20156 Milano
laura.vergani@polimi.it

ABSTRACT. The aim of this work is a review of scientific results in the literature, related to the application of thermographic techniques to composite materials. Thermography is the analysis of the surface temperature of a body by infrared rays detection via a thermal-camera. The use of this technique is mainly based on the modification of the surface temperature of a material, when it is stimulated by means of a thermal or mechanical external source. The presence of defects, in fact, induces a localized variation in its temperature distribution and, then, the measured values of the surface temperature can be used to localize and evaluate the dimensions and the evolution of defects. In the past, many applications of thermography were proposed on homogeneous materials, but only recently this technique has also been extended to composites. In this work several applications of thermography to fibres reinforced plastics are presented. Thermographic measurements are performed on the surface of the specimens, while undergoing static and dynamic tensile loading. The joint analysis of thermal and mechanical data allows one to assess the damage evolution and to study the damage phenomenon from both mechanical and energetic viewpoints. In particular, one of the main issues is to obtain information about the fatigue behaviour of composite materials, by following an approach successfully applied to homogenous materials. This approach is based on the application of infrared thermography on specimens subjected to static or stepwise dynamic loadings and on the definition of a damage stress, σ_D, that is correlated to the fatigue strength of the material. A wide series of experimental fatigue tests has been carried out to verify if the value of the damage stress, σ_D, is correlated with the fatigue strength of the material. The agreement between the different values is good, showing the reliability of the presented thermographic techniques, to the study of composite damage and their fatigue behaviour.

KEYWORDS. IR-thermography; Damage; Composite; Fatigue.

INTRODUCTION

Composite materials, widely used in structural applications for their well-known favourable strength-to-weight ratio, generally present a variety of defects or imperfections related to their heterogeneous nature and depending on the manufacturing process. Their mechanical properties, especially those of stiffness and strength, that are important in structural design, are connected to the presence defects. Dealing with cyclic loading, thus with fatigue problems, the assessment of structures and the prediction of residual life still remain an open issue in the literature. Also, the existence of a strength, which can be defined as fatigue limit for composite materials, is not even univocal. Some authors [1] do not find drastic change between low cycle fatigue and high cycle fatigue behaviour in composites, unlike in metals. On the

other side, other authors [2, 3] evidenced an infinite life region, where damage mechanisms are either arrested or prevented by a rather slow propagation rates to cause failure for large number of cycles.
All these problems dealing with fatigue of composites are complex, also because different kinds of damage can occur in these materials, leading to many kinds of failure modes: matrix cracking, fibre-matrix interfacial bond failure, fibre breakage, void growth, matrix crazing and delamination [4]. In order to detect damages in composite structures and to monitor their location and evolution during loading, adequate experimental techniques are therefore necessary. In the present review, among the available non-destructive techniques, infrared (IR) thermography is adopted. IR-thermography is a non-contact and non-destructive experimental methodology, based on the concept of surface temperature scanning during the application of a mechanical or thermal load on a structural component.
In the following, the paper gives an overview of the principles and methodologies at the basis of thermography as experimental non-destructive technique, especially dealing with composites. Different methods have been developed in the literature, initially applied to homogeneous materials, and recently applied also to composite structures. The attention is focused on the correlation between the thermal response of composites under mechanical loads, either static or dynamic, and the fatigue behaviour of the studied materials: the idea is to discuss thermographic methods and their applications in order to relate variations in thermal response to fatigue limit of composites.

INFRARED THERMOGRAPHY: PRINCIPLES AND APPLICATIONS

Infrared (IR) Thermography is a non-destructive technique, widely applied for quick inspection of large components. Laying on the principle that a grey body emits electromagnetic radiation due to its thermal conditions, IR-thermography allows performing contactless measurements of the surface temperature variation of the emitting body. This technique can be applied in a passive or active mode: the former is generally applied on materials, which experience a different temperature than the surrounding materials, the latter, instead needs an external stimulus to induce a surface temperature variation. The external stimulus can be a mechanical or a heat source. Passive thermography is rather qualitative, whereas active thermography allows both qualitative and quantitative analyses to be performed [5]. As qualitative analyses, this technique allows the detection of damages of various nature on different types of materials, e.g. fibre–matrix debonding and delamination in composites, moisture ingress in honeycomb sandwich materials, interfacial debonding in adhesive joints, crack-like defects in metals [6]. An example of thermography-based quantitative analysis instead, is the thermoelastic stress analysis (TSA), which is an experimental method of stress measurement based on the thermoelastic effect [7-12]. The thermoelastic effect, first described by Lord Kelvin [13] consists in the reversible temperature variation, occurring in a solid when it is deformed in the elastic field, and due to volume variation. This is summarized by the experimental equation of thermoelasticity, which states a linear relationship between the stress state of a homogeneous isotropic material in adiabatic conditions and its temperature variation:

$$\frac{\Delta T}{T_0} = -K_0 \, \Delta\sigma \tag{1}$$

where
- T_0 is the average temperature of the solid,
- $K_0=\lambda/\varrho C_p$ is the thermoelastic constant,
- λ is the linear thermal expansion coefficient,
- ϱ the mass density,
- C_p the specific heat at constant pressure
- $\Delta\sigma=\Delta(\sigma_1+\sigma_2+\sigma_3)$ is the variation of the first stress invariant.

This equation, formulated for a homogeneous isotropic material, has also been extended to orthotropic materials, by considering different thermoelastic constants in each direction, due to the anisotropy [14]. Indeed TSA, largely used for homogeneous materials, has also recently found application to orthotropic materials [10, 15]. However, in particular cases, such as for polymer composite materials, according to Salerno et al. [11] the thermoelastic constants have shown to be affected by the presence of a surface resin rich layer as well, which is few microns thick and creates a frequency dependence, by damping the thermal waves generated in the fibres. Nevertheless, surface temperature variations in materials do occur not only for thermoelastic effect, but also for irreversible transformations (i.e. damage, plastic deformation, and change in the microstructure).

Recent thermographic systems generally use an infrared detector, endowed with a sensor array, to measure the small reversible temperature changes, induced in a component, due to external stimuli, such as loads (e.g. in the case of TSA), or heat sources, such as pulsed light (e.g. in the case of pulsed thermography).

Thermographic techniques applied to composite materials

Many thermographic approaches are present in the literature to study behaviour of different composites, and to relate their thermal response to fatigue life, from almost 40 years. In the past, thermocouples were used, while, more recently, applications by means of IR-cameras connected with laptops for data acquisition have been developed. Moreover, dedicated softwares for thermal maps (matrices where the observed surface temperature is stored) handling have also been developed.

Considering tensile static loads, composites, as all other homogeneous materials, experience an initial decrease in surface temperature: this is due to the well-known thermoelastic effect [13] And it is related to the variation in volume during the elastic stage. Generally, after the initial decrease in temperature, while load increases, temperature deviates from linearity, till a minimum, then it starts to increase. A schematic of the classic stress trend and temperature trend is given in Fig. 1.

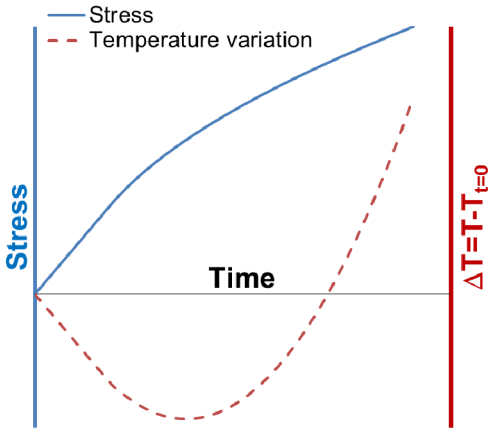

Figure 1: Schematic representation of the typical stress and temperature trends as a function of time, during a static tensile test.

From these experimental observations, some authors related the end of the thermoelastic stage to the fatigue limit of homogeneous materials [16], or to composite fatigue strength. This value of stress was named σ_D, where D stands for damage initiation. This idea was developed for glass [17, 18] and for basalt fibre reinforced composites [19]. In both these cases, if the applied load is lower than σ_D, defects present in the materials do not propagate and the global temperature trend during tensile static tests is linear. This was also confirmed by SEM analyses on glass-fibre reinforced specimens tested at various load levels [18] and by measurements of stiffness reduction in interrupted static tests charaterised by two loading-unloading cycles.

Together with this application of thermography to static tensile tests, also dynamic loads can be taken into account, and considerations on surface temperature changes can be proposed. From experimental observations [20], it was clear that during fatigue the surface temperature of the loaded specimens tends to reach a constant value, characteristic of the stress level. Also, the initial thermal response to cyclic (dynamic) loads, that is the increase of temperature (ΔT) during cycling (ΔN), thus the ratio $\Delta T/\Delta N$, is a typical feature of each tested material and it can be related to the applied stress. According to the literature, values of $\Delta T/\Delta N$, plotted as a function of different applied stresses, present a double linear trend [20]. The intercept between these two lines (i.e. the breakup point) identifies a stress level, which was experimentally found to be close to the fatigue limit. This experimental observation was confirmed not only for homogeneous materials, but also for composites [17, 19]. A schematic of the trend $\Delta T/\Delta N$ vs. maximum stress amplitude is given in Fig. 2.

A third method, based on progressively increased stress amplitudes and on energetic observations, was also proposed in the literature [21]. It is well known that dissipation of heat, thus energy, occurs when the material starts being damaged. This irreversible loss of energy is related to friction inside the material or to irreversible damage evolution. In [21], a new digital processing technique, called D-mode, is proposed to evaluate the dissipated energy. This technique can be performed with lock-in thermographic systems [22]. It extracts non-linear coupled thermo-mechanical effects during cycling. Dissipated energy is much smaller than thermo-elastic source and, therefore, the measure of this quantity requires a high sensitive thermal imaging camera. Its evaluation also requires a dedicated algorithm, which separates the dissipated energy from the thermo-elastic source and filters signals, neglecting the background noise. According to experimental

observations by Brémond [21], in case of progressively increased stress amplitudes, the dissipated energy shows a bi-linear trend. When the stress amplitude is low, the dissipated energy as a function of applied stress shows an almost flat trend, thus no energy is dissipated by irreversible mechanisms. Then, a rapid increase in the slope occurs for higher stress amplitudes, as schematically shown in Fig. 3, where a classic D-mode signal vs. stress amplitude trend is given. The author proposed that this breakup stress in the dissipated energy trend corresponds to a different behaviour in the material damage and indicates damage initiation in the material subject to dynamic loads. Thus it could be correlated with the material fatigue limit. This consideration has recently been validated also for carbon fibre reinforced composites [23, 24].

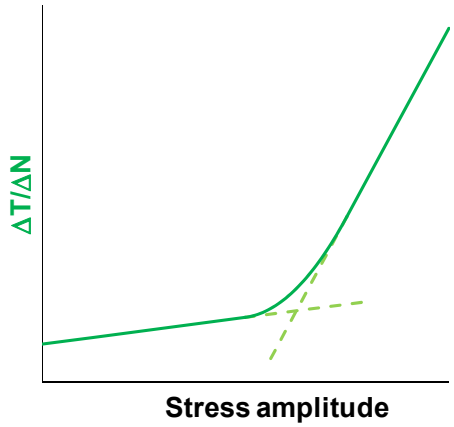

Figure 2: Schematic representation of the classic ΔT/ΔN trend with respect to the stress amplitude.

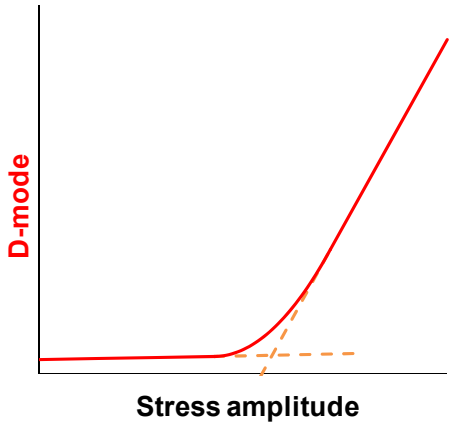

Figure 3: Schematic representation of the typical D-mode trend as a function of the stress amplitude.

MATERIALS

In our research studies we considered different materials, to investigate different damage types. Indeed, in the case of composite materials, it is interesting to probe the effects of the material internal organization on the mechanical response and on the damage modes.

We mainly focused on fibre-reinforced composites (FRC) made of natural or synthetic fibres, impregnated into polymer matrix, and arranged in different stacking sequences. In particular, in [18] we considered two E-glass/epoxy laminates with a 50% wt. of E-glass fibres (600 mg/m^2), obtained by manual lamination: one laminate made of unidirectional (i.e. UD) fibreglass, and one plate made of non-crimp fabrics (NCFs), with the following layup $[\pm 45°]_{10}$. From the composite plates we cut rectangular specimens and we placed GFRP adhesively bonded tabs at the specimen ends, as required by the standards [25, 26], ensuring a correct load transfer and avoiding any stress concentration due to the pressure applied in the grip zone. The dimensions of the specimens were also chosen according to the standards. We cut the UD-plate in two orthogonal directions, to get $[0°]_{10}$ and $[90°]_{10}$ stacking sequences. Also, to study the influence of defects in composites, we considered another plate of NCF-E-glass/$[\pm 45°]_{10}$ and we included a Teflon (PTFE) sheet, during the manufacturing process, to simulate a delamination damage and possible damage initiation sites [27]. Teflon layer was placed in correspondence of the middle layer: in this case, thermography was applied in order to localize a pre-existent damage and monitor its evolution during static or dynamic loads, as well as to evidence its influence on the surrounding regions. For this series of specimens, fibre content is 55% wt.

Another example of the application of thermography to composite materials is described in [19] and deals with basalt fibre reinforced plastics. In this work, basalt biaxial fabrics were used to manufacture laminated plates by vacuum infusion process and an epoxy resin, with stacking sequence $[0°/90°/+45°/-45°]_{2s}$ and a fibre content of 50% vol.

METHODS

Before performing thermal analyses we characterized all the materials under static loading conditions to determine the mechanical properties. Then, we used a thermal camera to monitor most of the performed tests. The camera is a FLIR Titanium IR-thermal camera, working in the waveband 2-5mm, with a 320·256 Focal Plane Array sensor, InSb cooling system and a 25mK thermal sensitivity. The adopted IR-camera is also endowed with a lock-in amplifier,

which amplifies the signal and filters the background noise, and a lock-in software, which operates a Fourier transform of the signals. This module is useful in case of a sinusoidal source, either mechanical or thermal. Indeed, by analysing a sequence of thermal images, acquired during a modulated cycle, it allows the measurement of the peak-to-peak temperature change, in terms of phase and amplitude, with respect to the modulated input cycle.
During the IR-monitored tests, we placed the IR-camera approximately 300mm far from the specimen surface. We scanned the central area of the specimens, since the heat transfer from the grips could have affected the upper and lower parts of the specimen. We connected the camera to a computer, for data analysis, and to the testing machine, to have a reference signal. Then we used Altair, the software of the thermal camera, to post-process the data. This software allows one to have full field thermal maps of the scanned surface, hence a quick damage detection, and to perform a pixel by pixel analysis of the temperature data.
Besides static and dynamic characterizations of the above described materials, we carried out different types of tests, under static and dynamic loading, coupled with thermal measurements. In particular, we performed:
i) static tests under monotonic loading,
ii) static tests with interrupted loading,
iii) stepwise dynamic tests.
For the static tests we followed the standards ASTM D3039/D 3039M-08 [25] for UD specimens and ASTM D 3518/D3518M-94 [26] for the specimens with ±45° fibres. Tests were performed in displacement control mode, under monotonic loading, using an MTS Alliance RF150 universal tensile testing machine with a 150 kN load cell. We chose a crosshead speed of 2 mm/min. During the tests, the surface temperature of the specimens was recorded by using the previously described thermal camera. The data acquisition frequency was set at 5 Hz for stress-strain data, and at 1 Hz for the temperature data.
We also performed interrupted static tests, by stopping the load at different previously defined values. For these tests we used the same tensile testing machine used for the monotonic static tests, and the above described IR-camera for the thermal measurements. The data acquisition frequency was set at 5 Hz for stress-strain data, and at 1 Hz for the temperature.
We performed two loading-unloading cycles and we measured, after each test, the stiffness reduction, defined as D, to have a first damage parameter:

$$D = \frac{E_2 - E_1}{E_1} \% \tag{2}$$

In Eq. (2), D is the damage, E_1 is referred to the stiffness measured during the first load cycle and E_2 is referred to the stiffness measured in the second load cycle. We also performed interrupted static tests, at previously defined load values, with a single loading-unloading cycle. After the tests we cut the specimens and we analysed the cross sections by means of a scanning electron microscope (SEM) to assess the internal damage due to the applied load.
Stepwise dynamic tests consists of dynamic tests with an increased applied load. A schematic of the load history is given in Fig. 4a. These tests were performed in load control mode, with a stress ratio equal to 0.1, and the specimen surface temperature was monitored with the IR-camera. In this case we used an MTS 810 hydraulic machine with a 100 kN load cell. The load frequency was set at 20 Hz and the thermal data acquisition at 80 Hz. The stress range, the step height, the step length, and the number of steps depend on the studied material. We carried out two types of stepwise dynamic tests: *i)* characterized by short steps (i.e. 10^3 cycles for each load step), and *ii)* characterized by longer steps (i.e. $6 \cdot 10^3$ cycles for each load step) for the case of glass/epoxy specimens with ±45° oriented fibres. In both cases we increased the amplitude stress by 2 MPa steps.
In the short-step tests, the data were analysed by using the dissipation mode (i.e. D-mode), a tool of the thermal camera to measure the energy dissipated by the material under cyclic loading. Indeed, the thermographic system is endowed with full radiometric software for lock-in applications, allowing the heat dissipation of a component, under dynamic loads, to be assessed. These measurements can give important information regarding the involved damage mechanisms.
In long step tests, besides performing a D-mode analysis, the temperature was also measured. The aim of these tests, characterized by longer loading steps, was to find the stabilization temperature [20] of the material for different applied loads and the initial slope $\Delta T/\Delta N$ for each applied stress. Indeed according to La Rosa and Risitano, in homogeneous materials subjected to cyclic loads, it is possible to recognize a repeating temperature trend, characterized by three phases: an initial temperature increase, a plateau region and then a final further increase in temperature. This characteristic trend is given in Fig. 4b (represented with a continuous black line), along with a bi-linear trend consisting of phase I and II (represented with a black dashed line), characteristic of composites [17, 19].

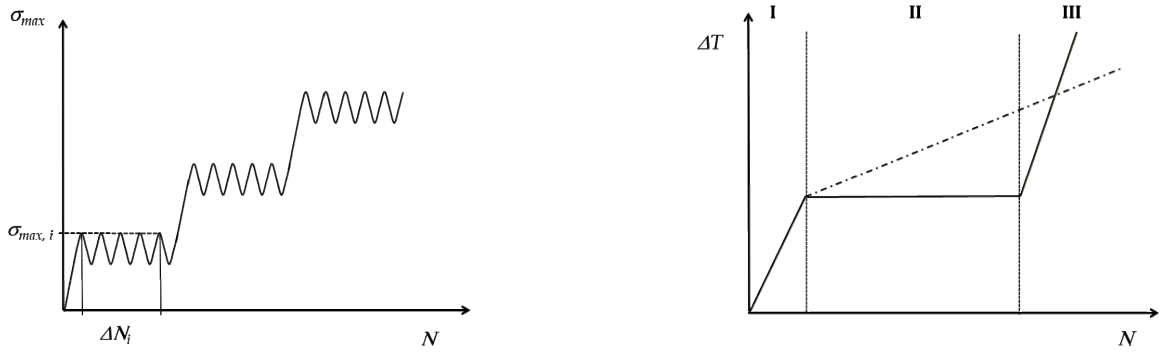

(a) (b)

Figure 4: a) Stepwise loading history. The characteristics of each interval (i.e. maximum applied stress and length of the interval) depend on the tested material. b) Thermal profile in each interval: the temperature characterized by an initial linear increasing region (I), represented with a black continuous line, then followed by a second linear region –represented by a back dashed line- or by a plateau region (region II, represented by a continuous black line) and a final increasing region (region II, represented by a continuous black line).

For basalt fibre reinforced composite in epoxy matrix, specimens were tested and subjected to blocks of 10000 cycles per step, and increasing stress amplitude of 10 MPa. Tests were stopped when the specimen failed.
As mentioned above, we also performed a fatigue characterization of the studied materials, by carrying out load-controlled dynamic tests according to the standard ASTM D 3479 [28]. For these tests we used an MTS 810 hydraulic machine with a 100 kN load cell, we set a stress ratio equal to 0.1 and a load frequency equal to 10 Hz.
We carried out tests at different load levels, to determine the σ_{max}-$LogN$ curve. In our initial studies we chose $5 \cdot 10^6$ cycles as the runout value, chosen as an average value from the literature. In a more recent study we also performed an HCF characterization, by setting the runout value at 10^7.
Then, in view of the obtained results, we made estimations about the materials damage initiation and growth, the materials failure mode, and the life of the materials.

CASE STUDIES

In this section, we show a series of case studies. We investigated the damage behaviour on glass fibre- and basalt fibre-reinforced composite materials; for the glass-FRC we also considered the effect of delamination. Here the results are shown on the basis of the type of performed test and analysis.
Generally with IR-thermography it is possible to perform both qualitative and quantitative analyses. Indeed, in our study by observing the thermal maps it was possible to locate damage, which appeared as the hottest region. The analysis of the thermal map during an entire test also allowed one to make hypotheses on the failure modes. For instance, during the tests some flashes of lighting were barely visible and oriented like the fibres of the tested materials, hence representing the energy release, due to debonding, at the fibre-matrix interface.
We also performed quantitative analyses, by accurately post-processing the thermal data. The temperature can be considered an important energetic parameter, strictly correlated to the damage state of the material. In our data analyses we measured the surface temperature and we averaged the temperature over the scanned area of each specimen, mainly corresponding to the central part of the specimen. Indeed, in our calculations we avoided the upper and lower parts of the specimen surface for the local influence due to the grips, and the external borders for the edge effect.
We should stress that the selection of the area, where to average the temperature data, has no influence on the results of the temperature trends. Indeed, we performed some trials, but the trends were globally similar, though upper or lower shifted on the temperature scale.

Static tests (continuous and interrupted) and microscopic analyses

The results of the static tests were repeatable for all the studied materials. Static tests allowed the determination of the mechanical properties of the materials. The thermal analyses allowed the study of the material behaviour from an energetic viewpoint.
In particular, a characteristic thermal trend has been found for all the materials and it is characterized by three regions:

1. An initial region, where the mechanical behaviour of the material is completely elastic, the mechanical energy is elastically stored by the material, and the temperature is approximately linearly decreasing.
2. A middle region, where the mechanical behaviour of the material is elastic from a macroscopic point of view, energy is absorbed in large part, and the temperature is nonlinearly decreasing, till a minimum. It is very likely that this region corresponds to the formation of local micro-damages, from pre-existent defects. This was also confirmed by micrographic analyses by means of an SEM, as shown in a previous work (Libonati and Vergani 2013).
3. A final region, where damage is propagating and leading to final failure. Here the thermal trend is nonlinear: at beginning there is a damage localization and a local temperature increase, then as damage is growing and spreading over the sample surface, a general rise in surface temperature occurs. Being the increase in temperature correlated with the energy release due to damage, the increase rate is strictly correlated with the damage mode. Indeed, we observed a net increase for more brittle behaviour (e.g. the case of GFRP material with UD glass fibres parallel or orthogonal to the applied load) [18], whereas a more progressive increase in temperature (i.e. energy release) occurred for materials showing a more progressive failure mode (e.g. the case of GFRP material with glass fibres oriented at ±45° with respect to the loading direction) [18].

A schematic of the characteristic temperature curve, showing the three above described regions, is given in Fig. 5, along with a characteristic stress-time curve. Indeed, by overlapping the two curves in the same graph we could find the stress levels corresponding to significant damage (i.e. temperature) events.

The first phase is characterized by a linear trend, and the data were fitted with a regression line, in all the studied cases. In the regression analyses we chose the experimental data to get the maximum regression coefficient. The temperature level, which represents the deviation from the linearity, coincides with the beginning of the second region. In our studies we correlated the end of the first region, from the energetic point of view, to the end of the linear thermoelastic behaviour of the material, whereas from the physical viewpoint, it could represent the beginning of the first micro-damages, probably originated from pre-existing defects, in the studied materials. Indeed, there was no defect visible by bare eyes, and considering the stress-time curve, it was difficult to define the range where the material has a completely elastic behaviour. By considering the temperature-time curves we were able to define the end of the linear thermoelastic region, for all the studied materials, and by overlapping the temperature-time curve to the stress-time curve, we could determine the stress value, corresponding to the end of the linear thermoelastic phase. In our previous work, this stress value was defined as damage stress, σ_D [17-19]. The average values of σ_D, obtained per each sample type are reported in Tab. 1, along with the mechanical properties (e.g. UTS and fatigue stress).

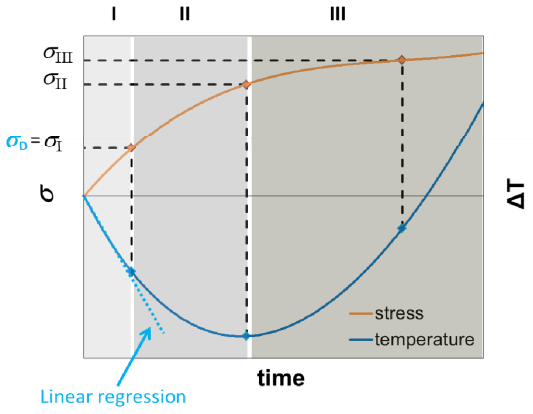

Figure 5: Schematic representation of stress and temperature trends and the three temperature regions, highlighetd with grayscale colors. In region I, the temperature data are fitted with a line, allowing the determination of the damage stress, σ_D, which corresponds to σ_I, the first stress level used in the interrupted static tests. In the graph, also σ_{II} and σ_{III} are highlighted, the former corresponding to the minimum temperature and to the end of region II, and the latter corresponding to the increasing temperature region (i.e. region III). Also, σ_{II} and σ_{III} are used as stress levels for the interrupted static tests.

The results of static tests, characterized by interrupted loading, were also interesting. The specimens were loaded until stress values corresponding to the end of the first and second temperature regions, and to a load level corresponding to the third region, in order to evaluate the material damage from a mechanical and physical point of view and to correlate the stress value corresponding to each temperature region with a mechanical damage parameter and an empiric observation. A schematic representation of these stress values (σ_I, σ_{II}, and σ_{III}) and the three temperature regions is given in

Fig. 5. In two loading-unloading cycle tests we determined the stiffness reduction as a mechanical damage parameter and we found that the damage parameter is negligible only when a specimen is loaded until a stress level smaller than the damage stress. Indeed, according to the results presented in [18], the tested material (i.e. E-glass/epoxy $[\pm 45°]_{10}$) seems not to be affected by the load application, until a certain load level, which corresponds to the damage stress, whereas for stress larger than the damage stress, non-negligible micro-damages are created into the material, leading to a deviation from the linearity in the temperature curve. These micro-damages, indeed, affect the mechanical performance, leading to a non-negligible stiffness reduction, in loading-unloading interrupted static tests. The material is macroscopically in the elastic field, but according to the thermal analysis, it is very likely that small damages originate from pre-existing defects.
In single loading-unloading cycles we investigated the damage state by analysing the cross sections of tested specimens by means of an SEM. Also these observations confirmed the hypotheses of the authors: stresses smaller than the damage stress σ_D cause a negligible damage, as stated by the small value of the damage parameter and by the SEM micrographic images, showing no stress-induced damage. The loading-unloading curves and the SEM images are given in [18].
Dealing with specimens of the same nature, reinforced in glass fibres oriented at ±45°, we observed that the presence of a delamination in the thickness does not induce variation in the mechanical properties, leading to an estimation through thermographic static method very similar to the one - above described - for undamaged specimens. Moreover, thermography applied following this approach did not lead to a clear localization of the defect. Decrease/increase in temperature is uniform on the specimen surface during the static test. Also, magnifications at the optical microscopy identified a uniform damage occurring in the specimens thickness [27].
For basalt reinforced, in [19] results dealing with basalt reinforced specimens in epoxy resin were reported, plotting temperature and stress data as a function of test time. A clear initial trend of the temperature was detected, till a minimum, which corresponds to a stress value very close to the one causing final failure.
For the case of basalt fibre reinforced composites in epoxy matrix, the end of the temperature linearity corresponds to 69 MPa (σ_D). It is likely that this value of stress, if compared to the fatigue results, indicates the fatigue limit of the material.
For a full comparison of the thermo-mechanical behaviour of these materials, in the present review all the results dealing with the previously discussed composites are reported, and a final plot is presented in Fig. 6. This graph shows, as a summary of all the presented test cases, a comparison among thermal answers of these different materials, as a function of the applied stress. These experimental data can be fitted by a line, thus identifying a ratio (slope) characteristic of each material. Considering these slopes, glass fibre composites resulted the ones cooling less quickly. This consideration is valid both for undamaged and delaminated specimens.

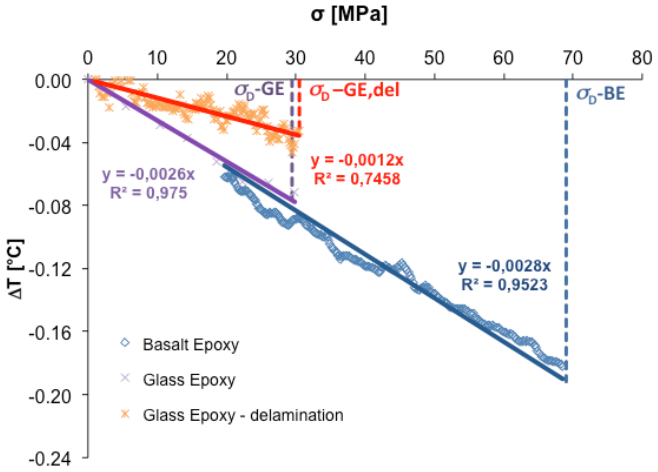

Figure 6: Temperature vs Stress for fibre reinforced composites: glass/epoxy, glass/epoxy with induced delamination, and basalt/epoxy. In this graph, only the data related to the linear temperature region (region I) are reported, along with the corresponding regression line. On the abscissa, the damage stresses of each tested material (σ_D-GE for glass/epoxy, σ_D-GE,del for glassy/epoxy with induced delamination, and σ_D-BE for basalt/epoxy) are highlighted.

Taking into account, instead, epoxy resin reinforced in basalt, the slope is higher and clearly different with respect to the cases of glass fibre composites. Moreover, in case of fibreglass the linear region ends up very early, while basalt composite presents a completely different behaviour showing higher estimation of fatigue performances (σ_D) [19].
This kind of plot, shown in Fig. 6, can be used to compare the global thermo-mechanical response of different materials. Even if it is obtained from experimental observations on static tests, this plot is extremely useful for mechanical design,

since it can offer quick information about fatigue behaviour of the materials, and in particular to their fatigue limit, or to a stress level corresponding to a different damage mechanism.

Dynamic tests (stepwise and fatigue)

The post-processing of the results obtained from the dynamic stepwise tests confirmed the hypotheses put forth, by observing the results of static tests.

In the case of E-glass/epoxy material, $[\pm 45°]_{10}$, the results obtained by stepwise dynamic tests, characterized by shorter and longer steps, were respectively analysed by measuring the D-mode signal and the $\Delta T/\Delta N$. In particular, by plotting the results of $\Delta T/\Delta N$-σ_{max} and D-mode-σ_{max} we get a bilinear trend, similar to the characteristic trends reported in Fig. 2 and Fig. 3, respectively. The breakup point was found to be 36 MPa. In Tab. 1 the average value of σ_D, (34) obtained from static and dynamic thermographic methods, is reported.

Instead, a net variation in the thermo mechanical response specimens is detected in delaminated samples tested by stepwise dynamic tests [27]. For these specimens, indeed, fatigue behaviour is deeply influenced by the presence of the localized damage in the thickness. This is clearly visible from experimental fatigue tests (Fig. 7).

Fig. 7 shows all the fatigue data available for the considered materials in a normalised S-N curve. In order to have comparable values along vertical axis for all the composites, the ratio between applied stress amplitude and ultimate tensile strength for each material is taken into account. Experimental fatigue data are fitted by means of straight lines, one for each material, to describe the finite life region. Considering the final part of the curve, related to the high cycle fatigue, thus fatigue limit, data of broken and runout specimens of all the considered composites show a flattening trend at approximately 20% of the ultimate tensile strength. This ratio seems a feature for all the composites, able to describe their fatigue strength.

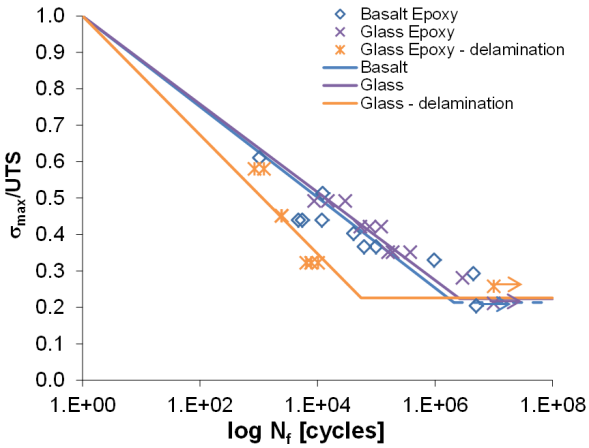

Figure 7: Normalized fatigue curves for all the materials. A linear interpolation is added in the finite life region, and the fatigue limit is plotted in the infite life region.

Material	Layup	Fibre content	UTS	Fatigue strength	Damage stress	σ_D/UTS %
E-glass/epoxy	$[0°]_{10}$	50% wt.	388±4	-	226	58
E-glass/epoxy	$[90°]_{10}$	50% wt.	59±10	-	33	56
E-glass/epoxy	$[\pm 45°]_{10}$	50% wt.	142±3	35	34	24
E-glass/epoxy*	$[\pm 45°]_{10}$	55% wt.	155±5	40	37	24
Basalt/epoxy	$[0°/90°/+45°/-45°]_{2s}$	50% vol.	409±9	-	74	18
**Teflon insert in the mid-section of the material layup to mimic delamination.*						

Table 1: Characteristics and mechanical properties of the tested materials. Damage stress is the average value among those obtained from the different thermographic methods, except for E-glass/epoxy $[0°]_{10}$ and $[90°]_{10}$ where only the static thermographic method has been applied.

In Fig. 7, focusing the attention on the finite life region, we can notice a larger decrease in the mechanical properties of delaminated specimens, if compared with the undamaged ones. Indeed this kind of specimens clearly shows different mechanical fatigue properties with respect to the other undamaged materials. Instead, as previously mentioned, its high cycle fatigue limit is approximately the same: in [27] it is hypothesized that, at high cycling, active mechanisms of fatigue damage are different than for finite life region. Delamination is active only in this finite stage of S-N curve, while its presence is not influencing mechanical fatigue behaviour at low stress amplitudes. From microscopy magnifications, moreover, it is clear that the Teflon layer is active for the performed tests and cracks start their evolution in the composite from the two edges of this induced damage.
The results from the application of thermographic techniques evidenced, for both $\Delta T/\Delta N$-σ_{max} and D-mode-σ_{max} plots, a similar value of fatigue limit (σ_D), for the cases of delaminated fiberglass. This value, moreover, is very similar to the same undamaged material: this supports the thesis that the presence of delamination does not influence the fatigue limit, which can be defined as a characteristic feature of the material.
The results of stepwise dynamic tests, carried out on basalt reinforced specimens, lead to a clear bi-linear trend in both the considered plots (i.e. $\Delta T/\Delta N$-σ_{max} and D-mode-σ_{max} graphs) based on thermal observations. However, the $\Delta T/\Delta N$-σ_{max} method appeared underestimating the fatigue limit, while σ_D value from D-mode and energetic technique appeared to be more realistic as fatigue limit of the basalt reinforced composite [19].

CONCLUDING REMARKS

In this review, we presented the application of IR-thermography to different composite materials, in order to relate the thermal response of these materials to their mechanical behaviour, and in particular to the fatigue limit. Glass and basalt fibre reinforced composites were considered and a review of thermographic approaches was discussed. According to the literature, three main thermographic methods are applied to composites to quantify, through this technique, fatigue performances of these materials. One is related to thermographic observations during static tests, while the other two deal with the application of dynamic load, and are based on thermal and energetic considerations. In the present review, applications of this techniques are discussed and compared for the different materials (glass fibre reinforced composites, without and with an induced delamination, and basalt fibre reinforced composites). Thermography is therefore proposed as a valid experimental technique able to quickly estimate mechanical fatigue properties through thermal response of the materials.

NOMENCLATURE

C_p	specific heat at constant pressure
D	damage parameter, defined in Eq. (2)
E	elastic modulus (stiffness)
FRC	fibre-reinforced composites
IR	infrared
K_0	thermoelastic constant
T_0	average surface temperature of solid
TSA	thermoelastic stress analysis
N	number of cycles
NCF	non-crimp fabrics
UD	unidirectional
ΔT	variation in surface temperature with respect to the initial temperature, T_0
λ	linear thermal expansion coefficient
ϱ	mass density
σ_D	damage stress, from thermographic observations
σ_{max}	maximum applied stress during fatigue cycling
σ_1, σ_2, σ_3	principal stresses
σ_I, σ_{II}, σ_{III}	stress as defined in Fig. 5

REFERENCES

[1] Bathias, C., An engineering point of view about fatigue of polymer matrix composite materials, International Journal of Fatigue, 28 (2006) 1094-1099.
[2] Gamstedt, E. K., Talreja, R., Fatigue damage mechanisms in unidirectional carbon-fibre-reinforced plastics, Journal of Materials Science, 34 (1999) 2535-2546.
[3] Keller, T., Tirelli, T., Zhou, A., Tensile fatigue performance of pultruded glass fiber reinforced polymer profiles, Composite Structures, 68 (2005) 235-245.
[4] Wu, Y., Polymer Microscopy. Third Edition. Eds: L.C. Sawyer, D.T. Grubb, G.F. Meyers. Springer, New York; (2008). ISBN 978-0-387-72627-4. Microscopy and Microanalysis, 15 (2009) 265-265.
[5] Maldague, X., Theory and practice of infrared technology for nondestructive testing, Wiley (2001).
[6] Armstrong, K. B., Bevan, L. G., Cole, W. F., Care and repair of advanced composites. SAE International (2005).
[7] Dulieu-Barton, J. M., Stanley P., Development and applications of thermoelastic stress analysis, The Journal of Strain Analysis for Engineering Design, 33 (1998) 93-104.
[8] Quinn, S., Dulieu-Barton, J. M., Langlands, J. M., Progress in Thermoelastic Residual Stress Measurement, Strain, 40 (2004) 127-133.
[9] Dulieu-Barton, J. M., Emery, T. R., Quinn, S., Cunningham, P. R., A temperature correction methodology for quantitative thermoelastic stress analysis and damage assessment, Measurement Science and Technology, 17 (2006) 1627.
[10] Emery, T. R., Dulieu-Barton, J. M., Thermoelastic Stress Analysis of damage mechanisms in composite materials, Composites Part A: Applied Science and Manufacturing, 41 (2010) 1729-1742.
[11] Salerno, A., Costa, A., Fantoni, G., Calibration of the thermoelastic constants for quantitative thermoelastic stress analysis on composites, Review of Scientific Instruments, (2009) 80.
[12] Greene, R., Patterson, E., Rowlands, R., Thermoelastic Stress Analysis. In: Springer Handbook of Experimental Solid Mechanics, ed. W. N. Sharpe, Jr., (2008) 743-768.
[13] Thomson, W., On the thermoelastic, thermomagnetic, and pyroelectric properties of matter. Philosophical Magazine Series 5, 5 (1878) 4-27.
[14] Stanley, P., Chan W. K., The application of thermoelastic stress analysis techniques to composite materials, The Journal of Strain Analysis for Engineering Design, 23 (1988) 137-143.
[15] Emery, T. R., Dulieu-Barton, J. M., Earl, J. S., Cunningham, P. R., A generalised approach to the calibration of orthotropic materials for thermoelastic stress analysis, Composites Science and Technology, 68 (2008) 743-752.
[16] Clienti, C., Fargione, G., La Rosa, G., Risitano A., Risitano G., A first approach to the analysis of fatigue parameters by thermal variations in static tests on plastics, Engineering Fracture Mechanics, 77 (2010) 2158-2167.
[17] Colombo, C., Libonati, F., Vergani, L., Fatigue damage in GFRP, International Journal of Structural Integrity, 3 (2012)
[18] Libonati, F., Vergani, L., Damage assessment of composite materials by means of thermographic analyses, Composites Part B: Engineering, 50 (2013) 82-90.
[19] Colombo, C., Vergani, L., Burman, M., Static and fatigue characterisation of new basalt fibre reinforced composites. Composite Structures, 94 (2012) 1165-1174.
[20] La Rosa, G., Risitano, A., Thermographic methodology for rapid determination of the fatigue limit of materials and mechanical components, International Journal of Fatigue, 22 (2000) 65-73.
[21] Brémond, P., IR imaging assesses damage in mechanical parts: determining the fatigue limit of real structures under real operating conditions saves time. Photonics Spectra (2004).
[22] Breitenstein, O., Langenkamp, M., Lock-In Thermography: Basics and use for functional diagnostics of electronic components. Springer (2003).
[23] Montesano, J., Fawaz, Z., Bougherara, H., Use of infrared thermography to investigate the fatigue behavior of a carbon fiber reinforced polymer composite, Composite Structures, 97 (2013) 76-83.
[24] Minak, G., On the determination of the fatigue life of laminated graphite-epoxy composite by means of surface temperature measurement, Journal of Composite Materials, (2010).
[25] ASTM D3039/D3039M-08, Standard test method for tensile properties of polymer matrix composite materials, (2008).
[26] ASTM D3518M-94, Standard test method for in-plane shear response of polymer matrix composite materials by tensile test of a ±45° laminate, (2007).

[27] Colombo, C., Vergani, L., Influence of delamination on fatigue properties of a fibreglass composite, Composite Structures, 107 (2014) 325-333.
[28] ASTM D3479M-96, Standard test method for tension-tension fatigue of polymer matrix composite materials, (2007).